AJNR

Progressive brain failure after diffuse hypoxic ischemic brain injury: a serial MR and proton MR spectroscopic study.

A Falini, A J Barkovich, G Calabrese, D Origgi, F Triulzi and G Scotti

AJNR Am J Neuroradiol 1998, 19 (4) 648-652
http://www.ajnr.org/content/19/4/648

AJNR Am J Neuroradiol 19:648–652, April 1998

Progressive Brain Failure after Diffuse Hypoxic Ischemic Brain Injury: A Serial MR and Proton MR Spectroscopic Study

A. Falini, A. J. Barkovich, G. Calabrese, D. Origgi, F. Triulzi, and G. Scotti

Summary: The findings at sequential MR imaging and proton MR spectroscopy of a patient with profound hypoxic-ischemic brain injury are reported. The pattern of structural and biochemical changes observed closely reflected the known evolution of postasphyxic brain degeneration. Particularly noteworthy were the sharp decrease of cortical *N*-acetylaspartate in the acute phase, suggesting the severity of the neuronal insult, and the subsequent progressive increase of choline, paralleling the delayed degeneration of white matter.

The term "cerebral death" indicates the irreversible cessation of the function of the cerebrum, in contradistinction to the term brain death, which indicates death of the entire organ. Cerebral death can result from vascular, infectious, or toxic causes. One of the most common causes of generalized or global (1) hypoxic-ischemic brain injury leading to irreversible cerebral death is cardiac arrest, often initiated by a period of hypoxemia, which reduces cardiac output and cerebral blood flow (2).

We had the opportunity to serially study a patient with severe global hypoxic-ischemic brain injury using magnetic resonance (MR) imaging and proton MR spectroscopy in the acute, subacute, and chronic phases. The results of this study are reported herein.

Case Report

A 34-year-old woman experienced severe glottic edema during the induction of anesthesia for a cesarian section. She had suffered prolonged respiratory distress due to difficulties in intubation. Respiratory arrest was aggravated by temporary cardiac arrest, which was reversed with external cardiac massage and defibrillation. The total time elapsed from the onset of respiratory insufficiency to resuscitation was about 15 to 20 minutes. After intubation and resuscitation, the patient remained in a deep coma (vegetative state) until death, which resulted from a secondary pulmonary infection 2 months after the arrest.

MR imaging and MR spectroscopy were performed at 1.5 T. CT consisted of axial 5-mm contiguous images obtained without the use of iodinated contrast material. MR imaging consisted of 5-mm T1-weighted spin-echo (605/15/2 [repetition time/echo time/excitations]) and proton density– and T2-weighted spin-echo images (2500/15,90/1) obtained in the axial and sagittal planes. Proton spectra were acquired using point-resolved spectroscopic sequences (3) with a chemical-shift selective saturation sequence (4) to suppress signal from the water, using a long TE of 270. The spectra were obtained in two 8-cm^3 volumes of interest (VOI) positioned in the occipital cortex and in the left centrum semiovale. After peaks assignment, areas were measured to calculate metabolite ratios.

Day 2

Unenhanced CT scans showed diffuse brain swelling. Brain parenchyma was diffusely hypodense with a loss in differentiation between gray and white matter. MR images confirmed severe brain edema with initial bilateral transtentorial uncal herniation. Gyral swelling was associated with a T2 prolongation of gray matter in both cerebral hemispheres (Fig 1A) and in the cerebellar cortex (mainly posterior hemispheres and superior vermis). T2 prolongation was also evident in the basal ganglia, particularly the caudate and lenticular nuclei.

Day 4

MR images showed a reduction of brain swelling with some expansion of the supratentorial ventricular system and a reversal of temporal lobe herniation. T2 prolongation of gray matter was still evident in the cerebral cortex, basal ganglia, cerebellar cortex, and superior vermis, with slightly less T2 prolongation in the occipital areas (Fig 2). MR spectra in the occipital cortex showed a markedly reduced *N*-acetylaspartate (NAA) peak with a slight increase of choline-containing compounds (Cho) relative to creatine (Cr) (Cho/Cr ratio) (Fig 3A). No significant abnormalities were evident in the VOI positioned in the white matter of the left centrum semiovale (Fig 3B).

Day 11

MR images showed significant brain atrophy. The cerebral cortex was thin, contrasting with the cerebellar cortex, which was still swollen and hyperintense. On T2-weighted images, hypointensity developed in the caudate nuclei and putamina (Fig 4A). The supratentorial white matter displayed T2 prolongation (Fig 4B), involving the corpus callosum, genu, and posterior limb of the internal capsules. Subcortical U fibers were spared. MR spectra in the occipital lobes displayed a

Received December 16, 1996; accepted after revision May 15, 1997.

From the Department of Neuroradiology, Scientific Institute San Raffaele Hospital, University of Milan (Italy) (A.F., G.C., D.O, F.T., G.S.), and the Department of Radiology, University of California San Francisco (A.J.B.).

Address reprint requests to Andrea Falini, MD, Neuroradiology Department, Scientific Institute S. Raffaele Hospital, Via Olgettina 60, 20132 Milan, Italy.

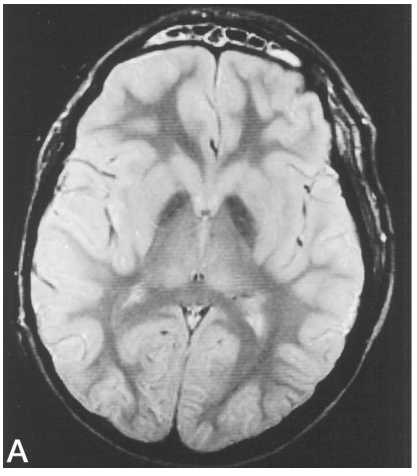

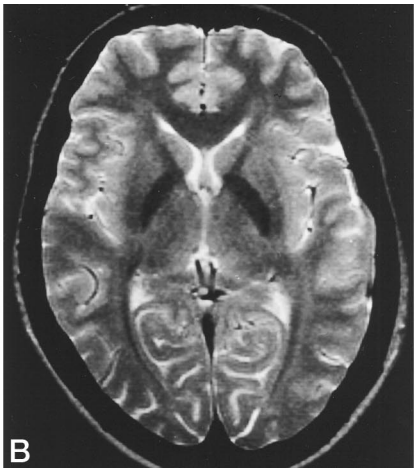

FIG 1. Axial T2-weighted (2500/90/1) MR image at day 2 after injury (*A*). The picture is dominated by massive edema involving both superficial and deep structures and by a dramatic T2 prolongation of gray matter in the cortex and in the deep nuclei. The increase in signal causes this T2-weighted image to resemble a proton density–weighted image; the signal modification is particularly evident as compared with an analogous axial T2-weighted image in a healthy subject (*B*).

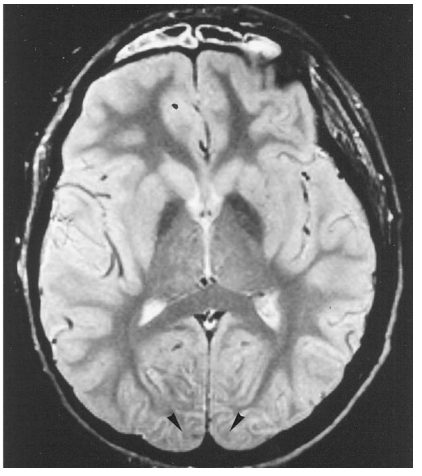

FIG 2. Day 4: MR imaging. T2-weighted image (2500/90/1) at the level of the basal ganglia shows a reduction of brain swelling and the persisting severe involvement of the cerebral cortex, which appears diffusely hyperintense. Hyperintensity of striatal structures (caudate and putamen) contrasts with lower intensity of less involved pallidal and thalamic nuclei. Occipital cortex edema seen in Figure 1 has partially resolved (*arrowheads*).

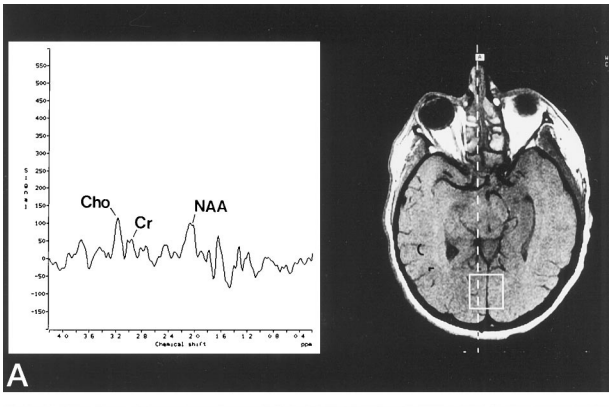

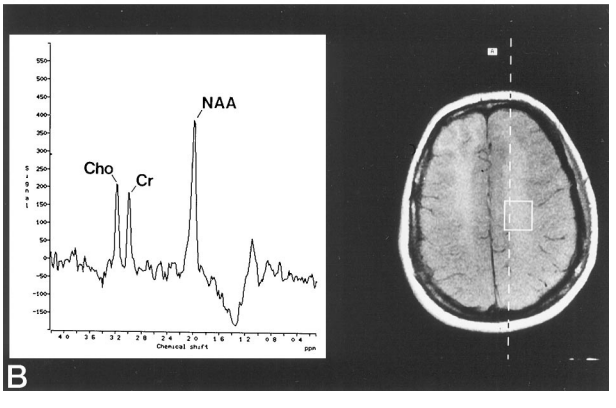

FIG 3. Day 4: MR spectroscopy.

A, In the occipital gray matter VOI, the NAA peak at 2 ppm is sharply reduced, suggesting severe damage to the neuronal population; Cho/Cr is slightly increased.

B, In the VOI positioned in the white matter, there are no significant spectral modifications, indicating a delay in the degenerative process of axons and myelin sheaths.

persistent depression of the NAA/Cr and NAA/Cho ratios and a slight increase in the Cho/Cr ratio. The white matter VOI revealed a sharp reduction of NAA with a normal Cho/Cr ratio.

Week 7

On MR images, profound atrophy had developed. The cerebral cortex was reduced to a thin layer. The deep gray nuclei were shrunken and showed decreased signal intensity, most pronounced in the striatum and least apparent in the thalami (Fig 5A). Atrophic changes in the cerebellum were less pronounced, involving mainly the posterior hemispheres and superior vermis. White matter exhibited increased T2 signal intensity in the subcortical and periventricular regions (Fig 5B). The MR spectroscopic pattern was very similar in both the gray (Fig 6A) and white matter (Fig 6B) VOIs, showing a reduced NAA peak and increased Cho/Cr ratios.

Discussion

The purpose of this study was to monitor the sequential alterations that occur in an adult after an acute hypoxic-ischemic brain injury using MR imaging and proton MR spectroscopy during the acute, subacute, and chronic phases, and to correlate the progressive imaging and metabolic modifications noted with the known pathologic events that follow this kind of brain accident.

In the present case, diffuse brain swelling, secondary to the failure of normal cellular energy metabolism resulting in impaired function of ion pumps, was the most prominent feature of the CT and MR studies obtained 2 days after the injury (Fig 1A). The brain edema involved superficial as well as deep structures, primarily the cerebral cortex and striatal nuclei. The more severe involvement of the neuronal

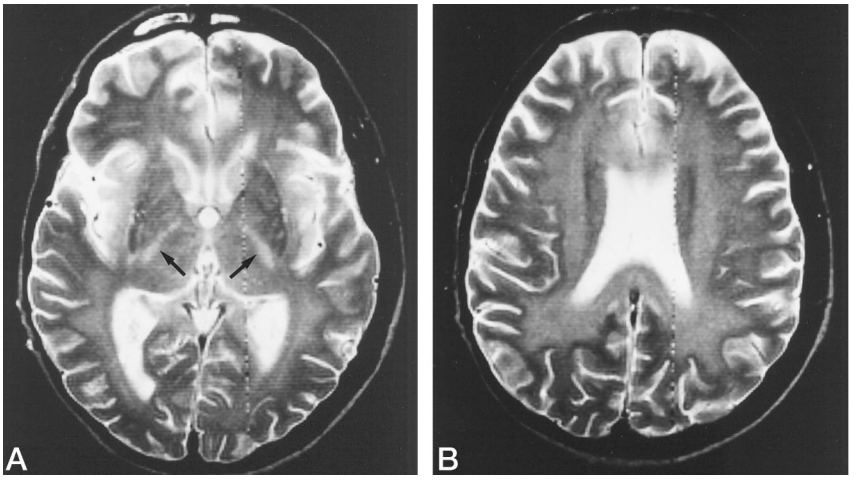

FIG 4. Day 11: MR imaging.

In addition to the evident brain atrophy, characterized by a thinned cerebral cortex and widened sulci and ventricular system, an axial T2-weighted image (2500/90/1) through the basal ganglia region (*A*) shows the persistent hyperintensity of the caudate nuclei and the progressive hypointensity developing in the putamina, reducing the usual differentiation with the globi pallidi. White matter injury is evident in the increased signal of the posterior limbs of the internal capsules (*arrows*) and, more clearly, in the higher section (*B*), in which a diffuse hyperintensity of the subcortical white matter (sparing the U fibers and the periventricular white matter, including the corpus callosum) is seen.

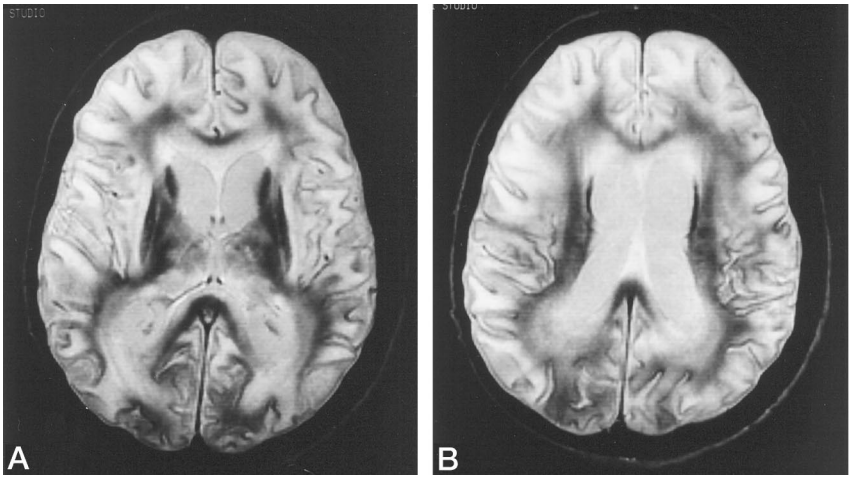

FIG 5. Week 7: MR imaging.

A, Axial T2-weighted image (2500/90/1) through the basal ganglia region shows massive degeneration involving cortical and deep gray structures. There is an ex vacuo enlargement of the ventricles and sulci; the cerebral cortex is reduced to a thin layer of hypointense gray matter. The basal ganglia are severely hypointense and shrunken.

B, The degenerative signals of the white matter are clearly appreciable, with an increased T2 signal intensity in the subcortical and periventricular regions, contrasting with a sharp hypointensity in the intermediate locations.

component stems from the concept of selective vulnerability (2). Neurons are known to be more vulnerable to oxygen deficiency than are oligodendroglia and astrocytes, while the microglia and the blood vessels are least vulnerable (5). Global brain ischemia due to cardiorespiratory arrest followed by reperfusion leads to typical alterations in the most vulnerable areas of the central nervous system. The selective involvement of the neocortex was more evident in the second study, performed on day 4, when brain swelling was largely reversed. The entirety of the cerebral cortex appeared deeply damaged. The reported existence of a gradient of neuronal involvement from a more compromised occipitoparietal area to the usually less compromised frontal and temporal regions (6) can be detected only in the observation of a more precocious evolution within the occipital cortex, with earlier resolution of edema. In addition, in our case, it is difficult to postulate a selective laminar damage due to the different resistance of cortical layers (among the cortical layers, the third is the most vulnerable, the fifth and sixth are somewhat less so, and the second and fourth layers are the most resistant) (2). Admittedly, observation of selective laminar necrosis on a standard MR image is likely to be difficult; moreover, the severity of the injury in this particular case makes it likely that all cortical layers were damaged. More evident are the differences in susceptibility between neurons of the phylogenetically older portions of the nervous system and the newer portions, the former being more resistant than the latter. Other than in the striking difference between the lesioned cerebral cortex and the largely spared gray nuclei of the brain stem, this phenomenon is best appreciated in the basal ganglia. While the caudate and putamen (neostriatal structures deriving from the telencephalon) were severely compromised, there was relative sparing of the globus pallidus and other diencephalic-derivative structures, like the thalami (Fig 2).

In our patient, MR spectra on day 4 reflected closely the process of neuronal death. The cortical VOI showed a reduction of NAA/Cho and NAA/Cr (Fig 3A), suggesting a depletion of NAA. The slight increase in the Cho/Cr ratio may reflect an increase of Cho, a reduction in Cr, or both. Choline prevalence may have resulted from the increase in the number of microglial cells (macrophages) that begins within 2 days (2), reflecting increased cellularity and membrane synthesis, and the contemporary neuronophagy (ie, phagocytosis of necrotic neurons) (2) with destruction and liberation of membranes (7). Creatine

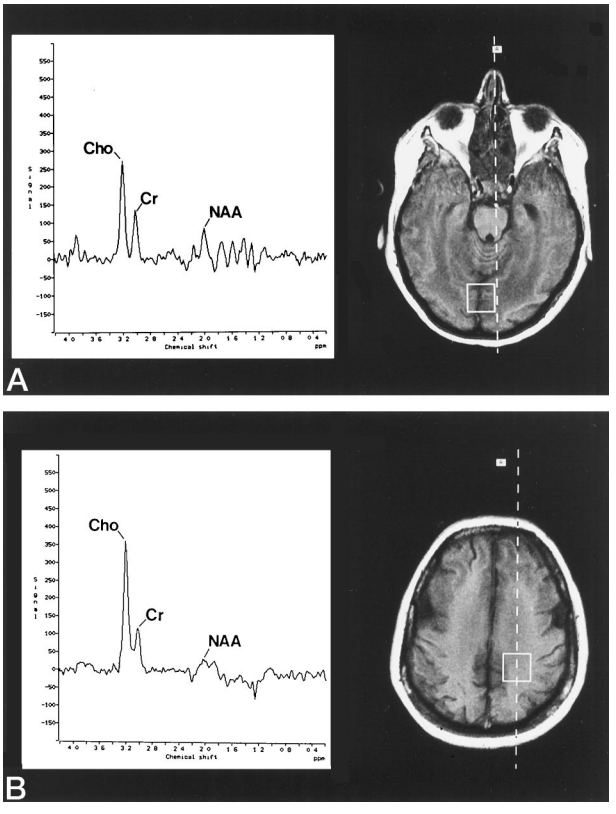

FIG 6. Week 7: MR spectroscopy.

MR spectroscopic data parallel imaging findings. The occipital gray matter (*A*) and the left centrum semiovale white matter (*B*) VOIs are characterized by a persistently depressed signal from NAA, expressing the depletion of neuronal components. An increased Cho/Cr ratio, probably caused by the final degradation of myelin associated with astrocytic proliferation, is present in both spectra, more pronounced in the white matter.

as a metabolic intermediate could be reasonably reduced in an ischemic area.

The normality of the white matter spectrum, also measured on day 4 (Fig 3B), is not surprising considering that it is known from the literature that axons may not degenerate until after 4 days and that axonal abnormalities precede changes in the surrounding myelin sheath (2). Moreover, there are differences in the rate of axon degeneration, depending on the axonal dimension. In young mammals, large axons show varicosities within 30 hours, while at 4 to 5 days they break up into fragments; however, thinner axons may not show the earliest cytologic abnormalities until after 10 days (8). This discrepancy between the cortical and white matter spectra on day 4 is important and emphasizes the need to include the cortex in the VOI of early postischemic brain spectra in adults (in neonates, the cerebral white matter is more metabolically active than the cortex, so spectra in neonates may evolve differently).

White matter changes became evident in our patient on the studies performed 11 days after ictus (Fig 4B). A delay in white matter compromise after a hypoxic event has been reported by other authors (9, 10) and temporally correlates with cortical damage (9). We can assume from the literature (11, 12) that at this time, day 11, most of the injured neurons were degenerated and that degeneration extended to axons and dendrites. Myelin sheath degeneration begins after axonal destruction. Structural alterations of the myelin sheath precede chemical degradation of myelin. The structural alterations result in a loosening of the lamellae (myelin vacuolization that can be responsible for the elongation of the T2 relaxation time) but the myelin sheath may not undergo frank degradation for 8 weeks or more (13). Daniel and Strich (14) found that baboon spinal cord myelin sheaths break up into ellipsoids within 48 hours but retain the staining properties of normal myelin for many weeks. Degeneration of tracts is associated with increased cellularity, present within 10 days, due to the greater number of astrocytic mitoses. After structural alteration takes place, chemical alterations follow, as protein and lipid break down into more basic constituents (14). The gap between neuronal and glial degeneration is clearly supported by MR spectroscopic results from our patient obtained during the subacute phase. NAA was depressed in the cortex, reflecting irreversible neuronal loss, and the Cho/Cr ratio was slightly augmented. More interesting, NAA was depressed in the white matter VOI, suggesting the extension of degeneration to the neuronal processes. The relative delay in myelin degradation, as compared with axonal degeneration, was observed in the normality of the Cho/Cr ratio, a sensible marker of membrane degradation.

The last study, following the hypoxic-ischemic insult by 7 weeks and shortly preceding the patient's death, showed dramatic changes in the imaging appearance of both gray and white matter. At this stage, atrophic changes dominated the picture. Neuronal loss, manifested as cortical thinning, was appreciated in the cerebral cortex, basal ganglia, and cerebellum, with a striking T2 hypointensity of the basal ganglia, probably reflecting the accumulation of paramagnetic substances in the neuronophagic cells (Fig 5A). The white matter signal showed a double pattern, with a sharp hyperintense T2 signal in the subcortical and periventricular regions and a sharp hypointense T2 signal in the intermediate areas of the corona radiata and centrum semiovale (Fig 5B). The sharp T2 hyperintensity could be related to both the demyelination process and the increased water content of the interstitial spaces, resulting from loss of vasoregulation. To explain the presence of hypointensity in degenerating white matter, Kuhn et al (15) argued that in the myelin breakdown process, myelin protein degradation occurs first; after proteins are broken down and cleared, uniform lipid structures remain chemically unaltered (14). From 4 to 14 weeks, lipid structures become relatively highly concentrated in tissue, water content being relatively diminished, resulting in the hypointense signal seen on T2-weighted images. Conversely, Takahashi et al (9) suggest that such signal loss may be due to increased iron deposition. This second hypothesis, which is supported by other evidence from MR imaging studies performed in young children with diffuse ischemic-anoxic brain in-

jury (16) and cerebral infarction (17), may be more likely in cases like the one presented here.

The MR spectra at 7 weeks paralleled the evolution of imaging studies. NAA/Cho and NAA/Cr levels showed no trend toward recovery in either VOI (Fig 6A and B), confirming the irreversible death of the major part of the neuronal population detected in the gray matter since the first study in the acute stage. The Cho/Cr ratio had increased progressively, mainly in the white matter (Fig 6B), probably reflecting the final stage of myelin breakdown associated with astrocytic proliferation.

In our patient, lactate was not observed in either of the regions studied during the acute, subacute, and chronic phases. This is in contrast with several previous reports describing the presence of lactate in acute and subacute ischemic areas. There are two possible explanations for our results: one is that lactate did not rise to a level detectable by MR spectroscopy, the other one is that we could not detect it.

Our patient suffered from an hypoxic-ischemic brain injury that selectively involved the neuronal population during early phases: this is a unique picture, very different from the experimental studies in which a single artery is temporarily ligated or hypoxia is artificially induced, or from studies performed in patients during strokes. A recent study in an animal model (18) showed that lactate almost disappeared 120 to 150 minutes after reversal of the hypoxia, and that ischemia alone did not cause any significant lactate production. In another study in children with severe acute central nervous system injury due to cardiorespiratory arrest (19), lactate was detected in two of six patients who were in a vegetative state or who had severe impairment at discharge. But the age of the patients varied from 0.25 to 42 months, and at this time the brain reacts to injuries in a way that is different from that in the adult. We can conjecture that, in our patient, the lactate was not detected in the acute phase owing to the prompt restoration of normal oxygen levels, while at day 11 its concentration was below the detectable level. After 7 weeks, the process of brain degeneration was at a chronic stage and the lack of lactate is less surprising. On the other hand, technical aspects must be considered. In an in vivo proton spectrum, lactate signal may be obscured by the presence of lipids. Membrane damage may lead to the release of free fatty acids and interfere with lactate (20). The presence of eddy currents can decrease the signal-to-noise ratio, making it even more difficult to see lactate. Moreover, variations in T1 and T2 relaxation times, observed in MR imaging studies, may alter the metabolite signal intensity in the spectrum.

Conclusion

Sequential MR imaging and MR spectroscopy of a patient with profound hypoxic-ischemic brain injury revealed a pattern of structural and biochemical changes that reflected the known process of postasphyxic brain degeneration. Particularly noteworthy was a sharp decrease of NAA in the acute phase, suggesting the severity of the neuronal insult, and a delayed wear damage of supratentorial white matter. Detection of such changes may prove helpful in the early evaluation of patients with such injuries.

References

1. Garcia JH. **Cerebral ischemia: the early structural changes and correlations of these with known metabolic and dynamic abnormalities.** In: Whisnant JP, Sandok B, eds. *Cerebral Vascular Disease, Ninth Conference.* New York, NY: Grune & Stratton; 1975:313–323
2. Graham DI. **Hypoxia and vascular disorders.** In: Adams JH, Duchen LW, eds. *Greenfield's Neuropathology.* 5th ed. New York, NY: Oxford University Press; 1992:153–268
3. Bottomley PA. **Spatial localization in NMR spectroscopy in vivo.** *Ann N Y Acad Sci* 1987;508:333–348
4. Haase A, Frahm J, Haenicke W, Matthei D. **1H NMR chemical shift selective (CHESS) imaging.** *Phys Med Biol* 1985;30:341–344
5. Jacob H. **CNS tissue and cellular pathology in hypoxaemic states.** In: Schade JP, McMenemey WH, eds. *Selective Vulnerability of the Brain in Hypoxaemia.* Oxford, Blackwell Scientific; 1963:153–163
6. Adams JH, Brierley JB, Connor RCR, Treip CS. **The effects of systemic hypotension upon the human brain: clinical and neuropathological observations in 11 cases.** *Brain* 1966;89:235–268
7. Frahm J, Bruhn H, Hanicke W, Merborldt KD, Mursch K, Markakis E. **Localized proton NMR spectroscopy of brain tumors using short-echo time STEAM sequences.** *J Comput Assist Tomogr* 1991;15:915–922
8. Ramon y Cajal S. ***Degeneration and Regeneration of the Nervous System.*** London, England: Oxford University Press; 1928
9. Takahashi S, Higano S, Ishii K, et al. **Hypoxic brain damage: cortical laminar necrosis and delayed changes in white matter at sequential MR imaging.** *Radiology* 1993;189:449–456
10. Ginsberg MD, **Delayed neurological deterioration in following hypoxia.** In: Fahn S, Davis JN, Rawland LP, eds. *Advances in Neurology.* New York, NY: Raven; 1979;26:21–44
11. Brown AW, Brierley JB. **The earliest alterations in rat neurones after anoxia-ischaemia.** *Acta Neuropathol* 1973;23:9–22
12. Brown AW. **Structural abnormalities in neurones.** *J Clin Pathol* 1977;30(Suppl 11):155–169
13. Garcia JH, Anderson ML. **Circulatory disorders and their effects on the brain.** In: Davis RL, Robertson DM, eds. *Textbook of Neuropathology.* 2nd ed. Baltimore, Md: William & Wilkins; 1991: 621–718
14. Daniel PM, Strich SJ. **Histological observations on wallerian degeneration in the spinal cord of the baboon, Papio P.** *Acta Neuropathol* 1969;12:314–328
15. Kuhn MJ, Mikulis DJ, Ayoub DM, Kosofsky BE, Davis KR, Taveras JM. **Wallerian degeneration after cerebral infarction: evaluation with sequential MR imaging.** *Radiology* 1989;172:179–182
16. Dietrich RB, Bradley WG. **Iron accumulation in the basal ganglia following severe ischemic-anoxic insults in children.** *Radiology* 1988;168:203–206
17. Cross PA, Atlas SW, Grossman. **MR evaluation of brain iron in children with cerebral infarction.** *AJNR Am J Neuroradiol* 1990;11: 341–348
18. Nakai T, Rhine WD, Enzmann DR, Stevenson DK, Spielman DM. **A model for detecting early metabolic changes in neonatal asphyxia by 1H-MRS.** *J Magn Reson Imaging* 1996;6:445–452
19. Ashwal S, Holshouser BA, Hinshaw DB, Schell RM, Bailey L. **Proton magnetic resonance spectroscopy in the evaluation of children with congenital heart disease and acute central nervous system injury.** *J Thorac Cardiovasc Surg* 1996;112:403–414
20. Howe FA, Maxwell RJ, Saunders DE, Brown MM, Griffiths JR. **Proton spectroscopy in vivo.** *Magn Reson Q* 1993;9:31–59